ISCI, Volume *13*

Supplemental Information

Alzheimer Aβ Assemblies Accumulate in Excitatory Neurons upon Proteasome Inhibition and Kill Nearby NAKα3 Neurons by Secretion

Hitomi Komura, Shota Kakio, Tomoya Sasahara, Yoshie Arai, Naomi Takino, Michio Sato, Kaori Satomura, Takayuki Ohnishi, Yo-ichi Nabeshima, Shin-ichi Muramatsu, Isao Kii, and Minako Hoshi

Supplemental Information

Supplemental Figures

Figure S1

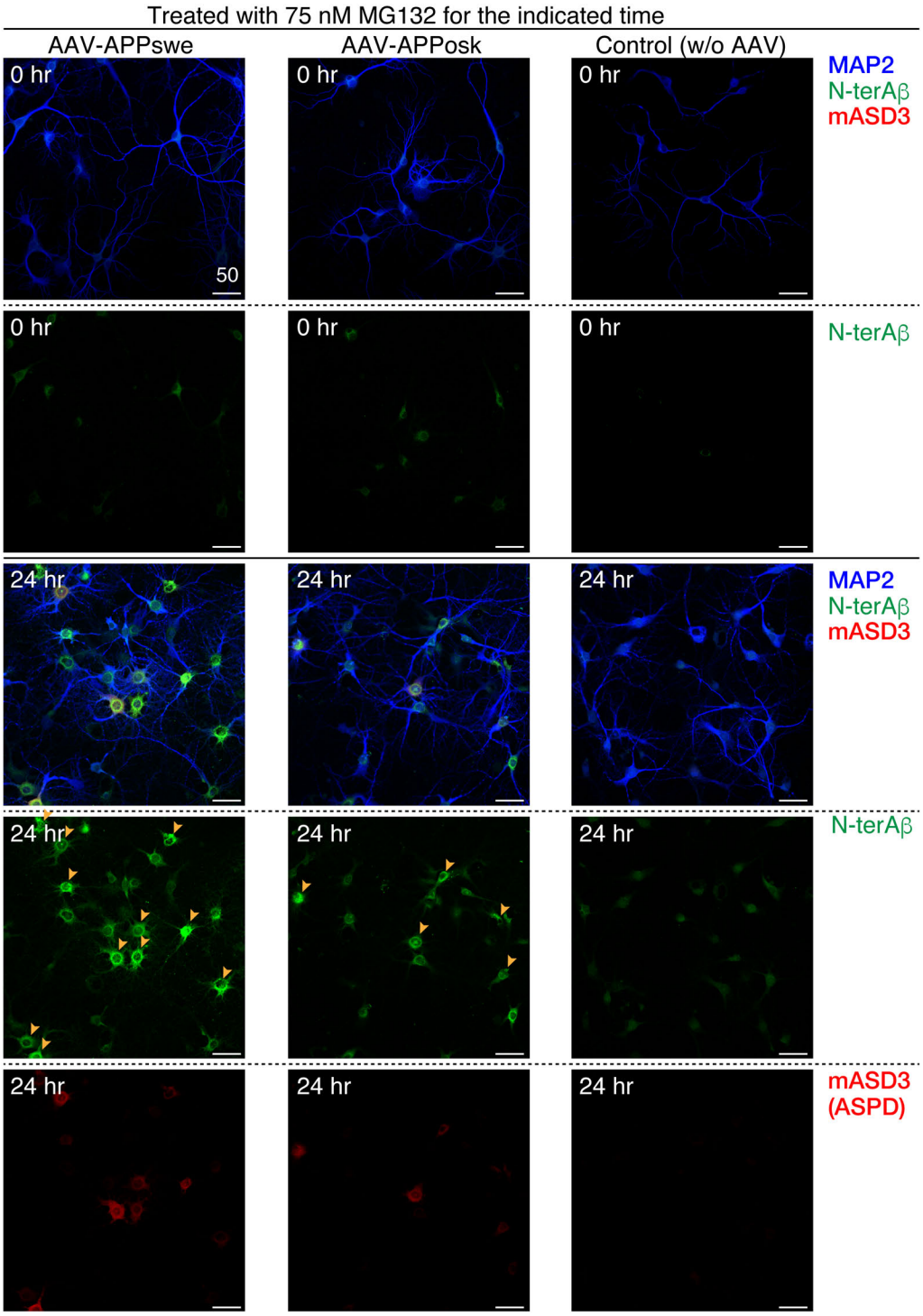

Figure S1 Effect of Proteasome Inhibition on Aβ and ASPD Accumulations, related to Figures 2, 4, and 11

Primary rat hippocampal neuronal cultures, with or without AAV-APP transduction, were treated with 75 nM MG132 for the indicated time. The cultures were triple-stained with antibodies against MAP2, Aβ N-terminal end (N-terAβ), and ASPD (mASD3). Representative images are shown. Single channel images of green or red are shown below. Scale bar = 50 μm. Arrowheads mark neurons with intense N-terAβ signals with ASPD staining.

Figure S2

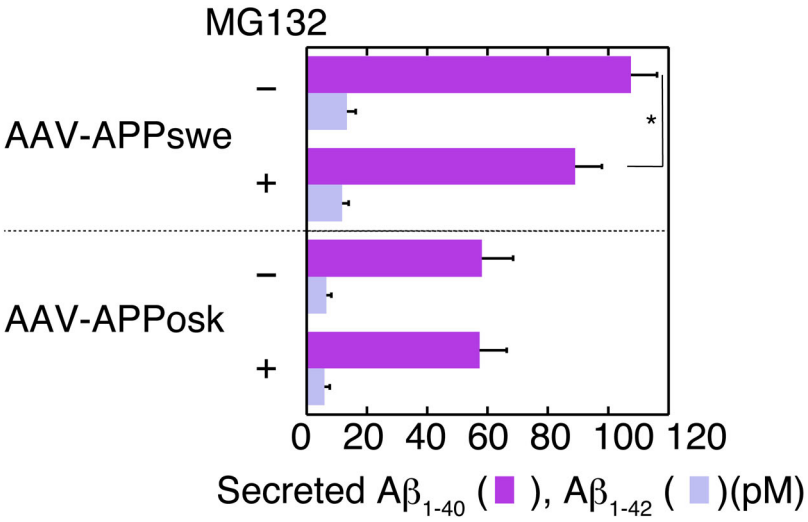

Figure S2 Proteasome Inhibition Does Not Affect Aβ Secretion, related to Figure 3

The culture supernates were obtained from APP-transduced primary rat hippocampal neuronal cultures, treated with or without 75 nM MG132 for 24 hr. $A\beta_{1\text{-}40}$ and $A\beta_{1\text{-}42}$ were quantified by using a WAKO ELISA system (Transparent Methods). (mean ± SD, n = 4; Scheffé *post hoc* test, *, $p = 0.04$)

Figure S3

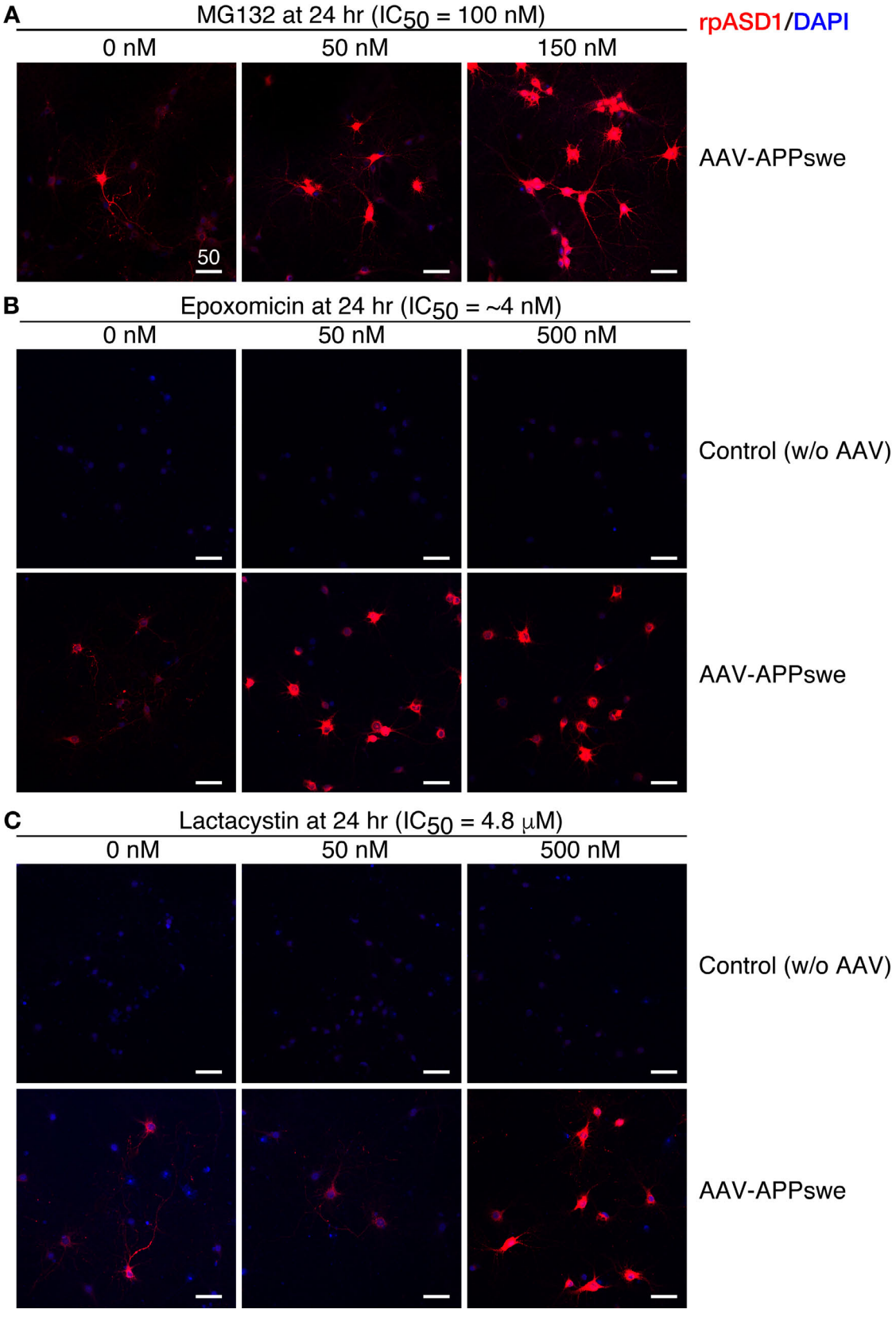
A
MG132 at 24 hr (IC50 = 100 nM)
rpASD1/DAPI
0 nM
50 nM
150 nM
50
AAV-APPswe
B
Epoxomicin at 24 hr (IC50 = ~4 nM)
0 nM
50 nM
500 nM
Control (w/o AAV)
AAV-APPswe
C
Lactacystin at 24 hr (IC50 = 4.8 μM)
0 nM
50 nM
500 nM
Control (w/o AAV)
AAV-APPswe

Figure S3 Effect of Mechanistically Different Proteasome Inhibitors on ASPD Accumulation, related to Figure 4

Primary rat hippocampal neuronal cultures, with or without AAV-APPswe transduction, were treated with MG132 (**A**), epoxomicin (**B**), or lactacystin (**C**) at the indicated concentration for 24 hr. The cultures were stained with anti-ASPD rpASD1 antibody and DAPI. Representative images are shown. Scale bar = 50 μm. All these proteasome inhibitors increased the neuronal ASPD staining at 24 hr, as shown in Figure 4A. The range of the dose-dependency of each inhibitor correlated reasonably well with the IC_{50} value.

Figure S4

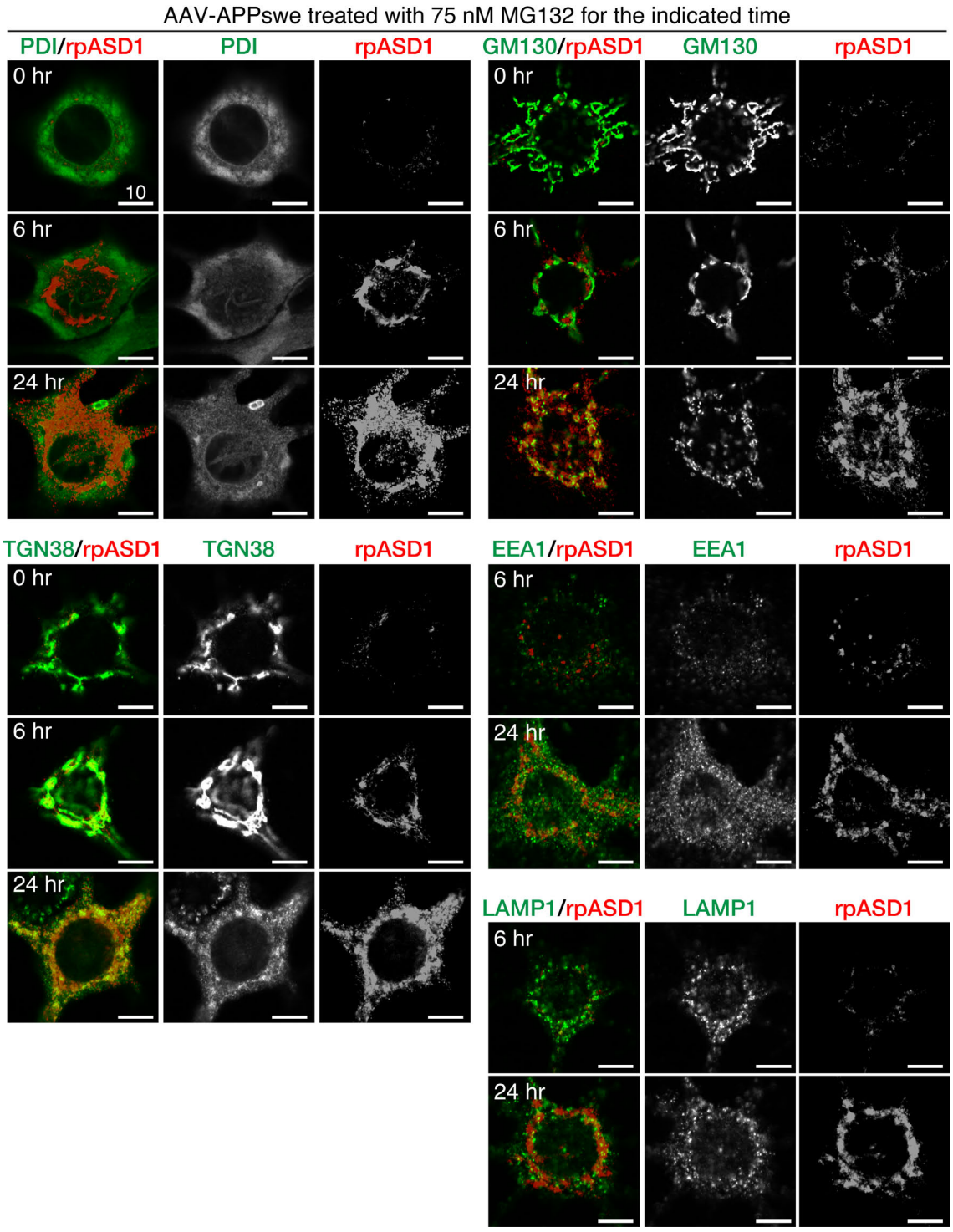

Figure S4 ASPD Accumulate in the Trans-Golgi of Mature Neurons, related to Figures 6 and 7

Primary rat hippocampal neuronal cultures with AAV-APPswe transduction were treated with 75 nM MG132 for the indicated time. The cultures were double-stained with anti-ASPD rpASD1 antibody and antibody against organelle marker protein (see Transparent Methods). Representative double-stained images obtained with a highly sensitive, direct photon-counting system with a 100x oil objective lens are shown, along with the corresponding single red or green images. Scale bar = 10 μm.

Figure S5

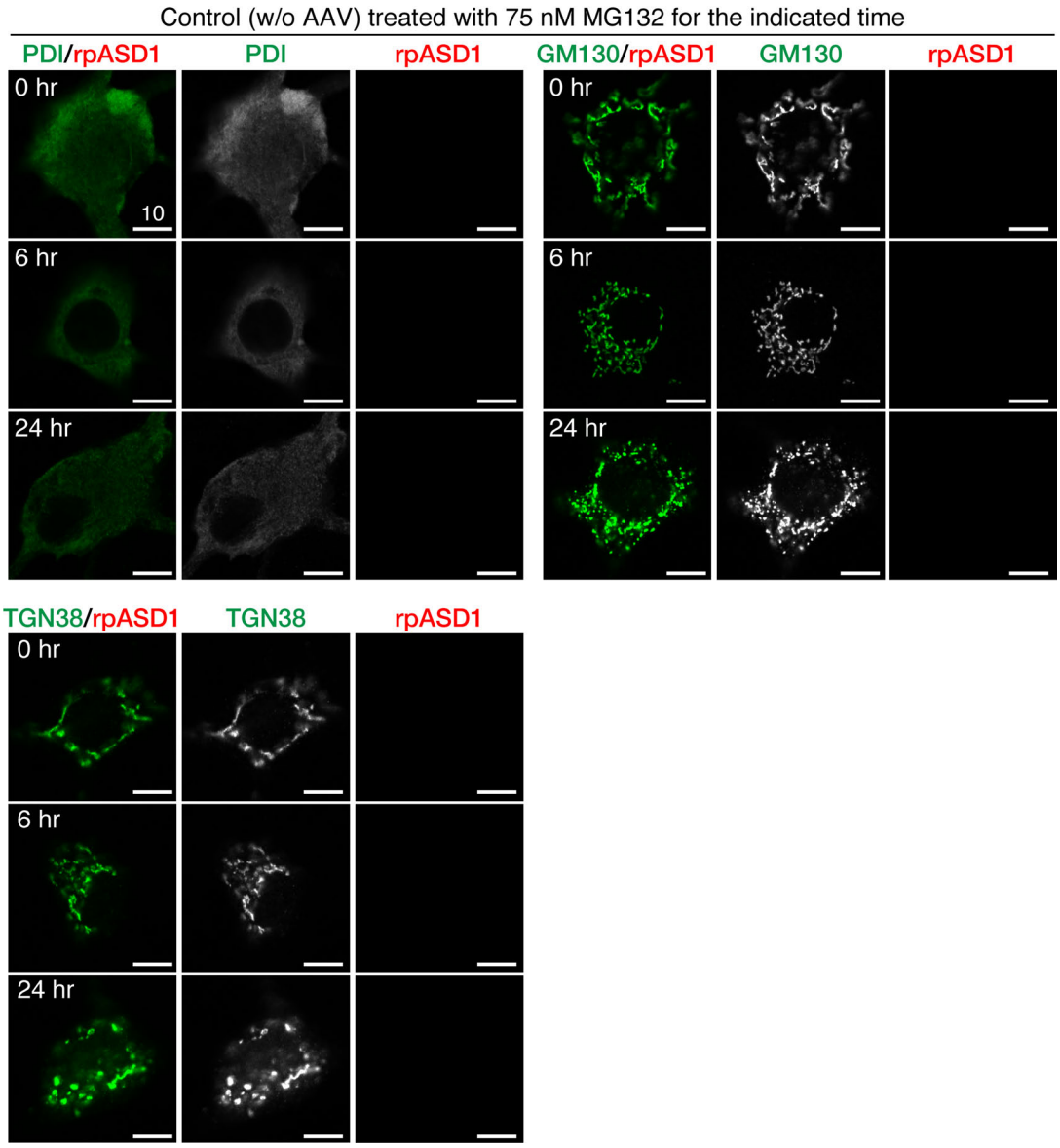

Figure S5 ASPD Rarely Accumulate without APP Transduction, related to Figures 6 and S4

Control experiment for Figure 6. Primary rat hippocampal neuronal cultures without AAV-APPswe transduction were treated with 75 nM MG132 for the indicated time and were double-stained with anti-ASPD rpASD1 antibody and antibody against organelle marker protein (see Transparent Methods) as in Figure 6. Representative double-stained images obtained with a highly sensitive, direct photon-counting system with a 100x oil objective lens are shown, along with the corresponding single red or green images. Scale bar = 10 μm.

Figure S6

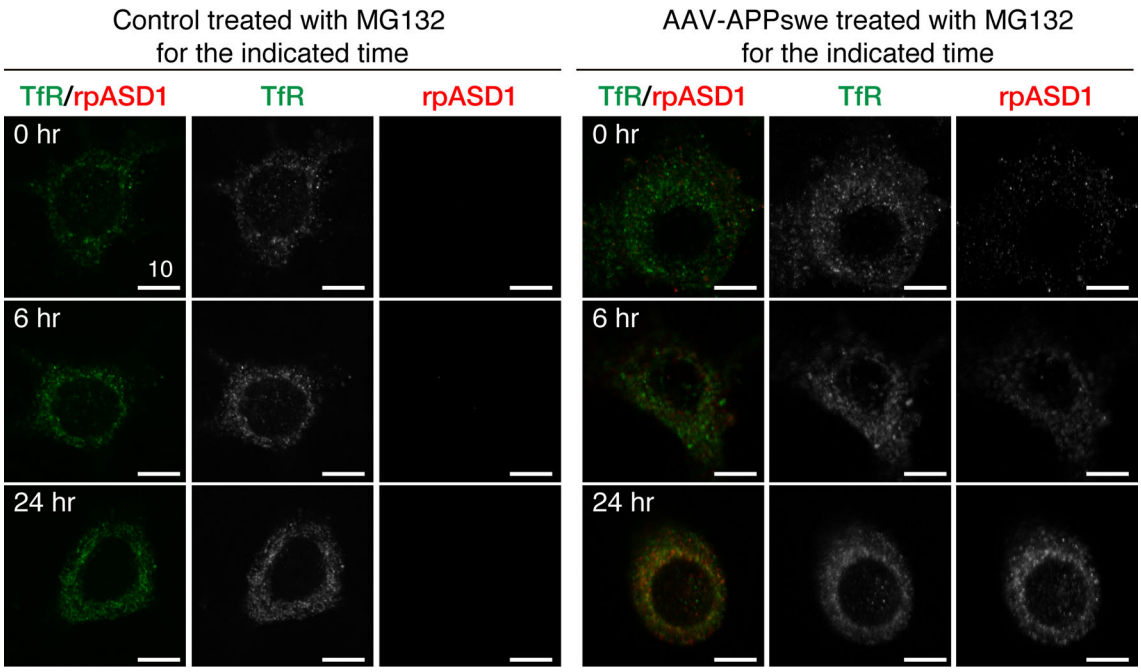

Figure S6 ASPD Accumulate in the Recycling Endosomes of Mature Neurons, related to Figure 8

Primary rat hippocampal neuronal cultures, with or without AAV-APPswe transduction, were treated with 75 nM MG132 for the indicated time. The cultures were double-stained with anti-ASPD rpASD1 and anti-TfR antibody (see Transparent Methods). Representative double-stained images obtained with a highly sensitive, direct photon-counting system with a 100x oil objective lens are shown, along with the corresponding single red or green images. Scale bar = 10 μm.

Figure S7

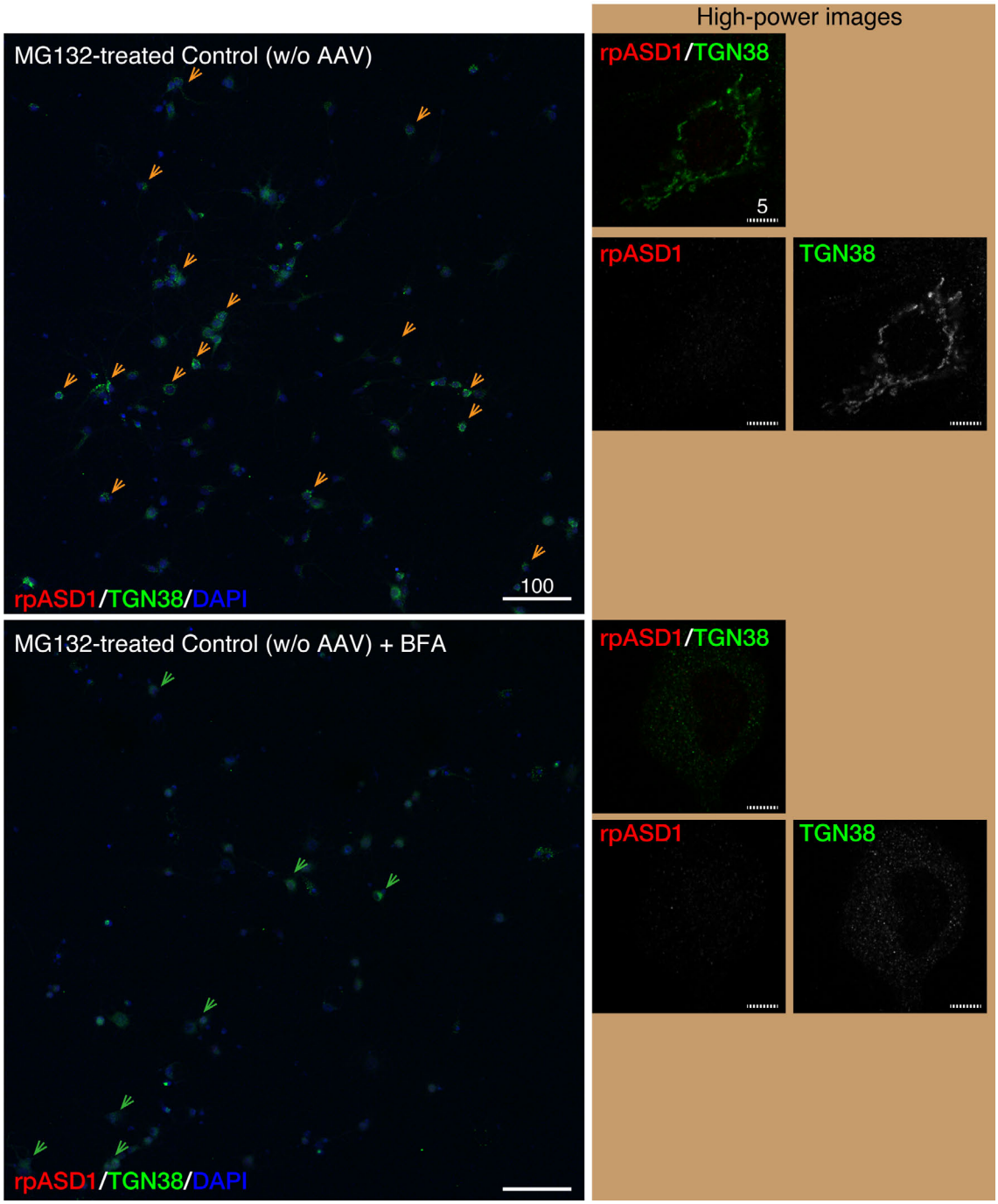

Figure S7 BFA Effects on the TGN in Control Mature Neurons, related to Figures 9 and S8

Control experiment for Figure 9 is shown. Primary rat hippocampal neuronal cultures without AAV-APPswe transduction were treated with 75 nM MG132 for 24 hr in the absence or the presence of 0.6 μg/ml BFA. The cultures were triple-stained with

rpASD1, anti-TGN38 antibody (TGN marker), and DAPI. Representative images are shown. Orange arrows mark neurons that still appear to retain the Golgi structure, while green arrows mark neurons that show collapsed TGN staining. TGN38 staining was lost or diffusely spread throughout the cytoplasm in untransduced cells treated with MG132 and 0.6 μg/ml BFA together, indicating that BFA collapsed the Golgi apparatus (green arrows and high-power images in the right). In contrast, the Golgi structure appeared to be still preserved in some neurons of untransduced cells treated with MG132 in the absence of BFA (orange arrows and high-power images in the right). High-power images obtained with a highly sensitive, direct photon-counting system with a 100x oil objective lens are shown on the right. Solid and hatched scale bars are 100 and 5 μm, respectively.

Figure S8

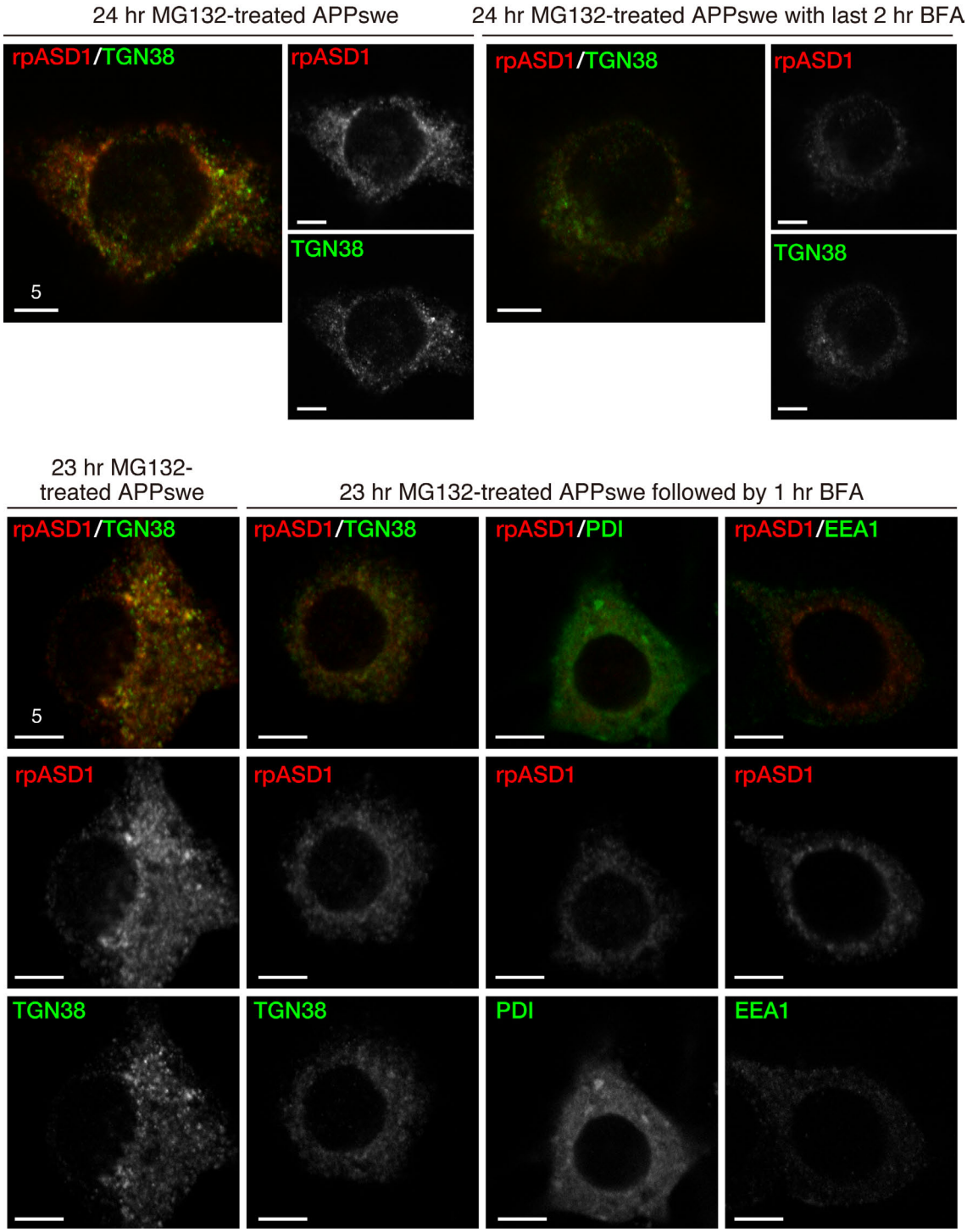

Figure S8 Effect of Brief BFA Treatment on the TGN in APPswe-Transduced Mature Neurons, related to Figures 9 and S7

Control experiment for Figure 9 showing the effects of brief treatment with BFA. APPswe-transduced primary rat hippocampal neuronal cultures were treated with 75 nM MG132 for 22-23 hr, followed by 0.6 μg/ml BFA treatment for another 1-2 hr. The cultures were triple-stained with rpASD1, an antibody against organelle marker protein, and DAPI. Representative images are shown. High-power images obtained with a highly sensitive, direct photon-counting system with a 100x oil objective lens are shown on the right. Scale bar = 5 μm. As shown in the images at 1 hr and 2 hr BFA treatment, the ASPD and TGN38 signals decreased substantially with increased duration of BFA treatment. In the case of 1 hr BFA treatment, ASPD signals still largely remained co-localized with TGN38 staining. However, more ASPD signals appeared in the ER, because BFA leads to retrograde transport from the Golgi apparatus to the ER (Nebenfuhr et al., 2002). In contrast, ASPD signals were only rarely co-localized with the EE, as was also observed before BFA treatment (see 24 hr EEA1/rpASD1 staining in Figure 6).

Figure S9

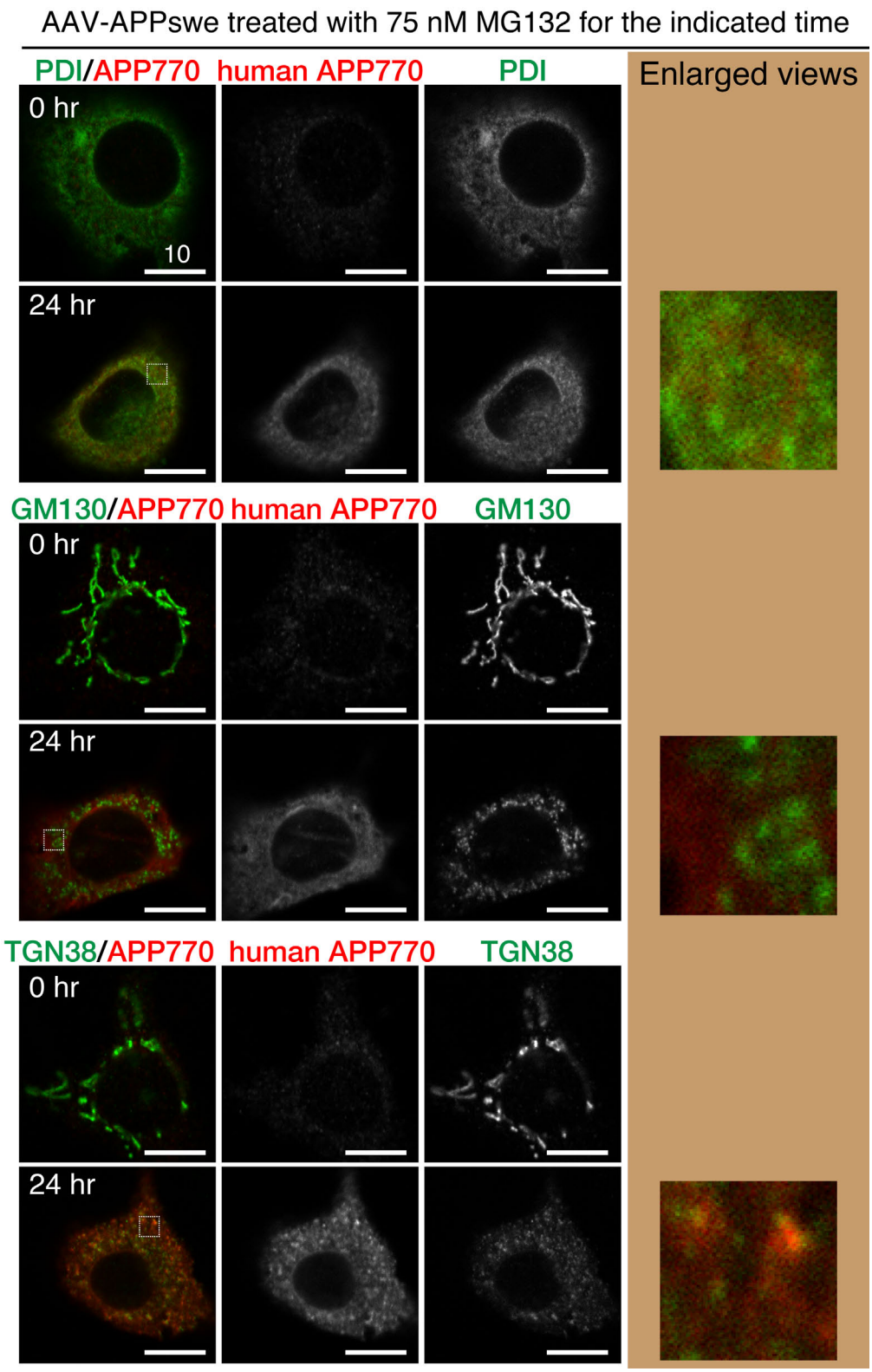
AAV-APPswe treated with 75 nM MG132 for the indicated time
PDI/APP770
human APP770
PDI
Enlarged views
0 hr
10
24 hr
GM130/APP770
human APP770
GM130
0 hr
24 hr
TGN38/APP770
human APP770
TGN38
0 hr
24 hr

Figure S9 Steady-State Distribution of human APP770, with or without Proteasome Inhibition, in APPswe-Transduced Mature Neurons, related to Figure 10

APPswe-transduced primary rat hippocampal neuronal cultures were treated with 75 nM MG132 for the indicated time. The cultures were double-stained with anti-human APP770 antibody and antibody against organelle marker protein (see Transparent Methods). Representative double-stained images obtained with a highly sensitive, direct photon-counting system with a 100x oil objective lens are shown, along with the corresponding single red or green images. An enlarged view of the field enclosed by a hatched line is shown on the right. Scale bar = 10 μm.

Figure S10

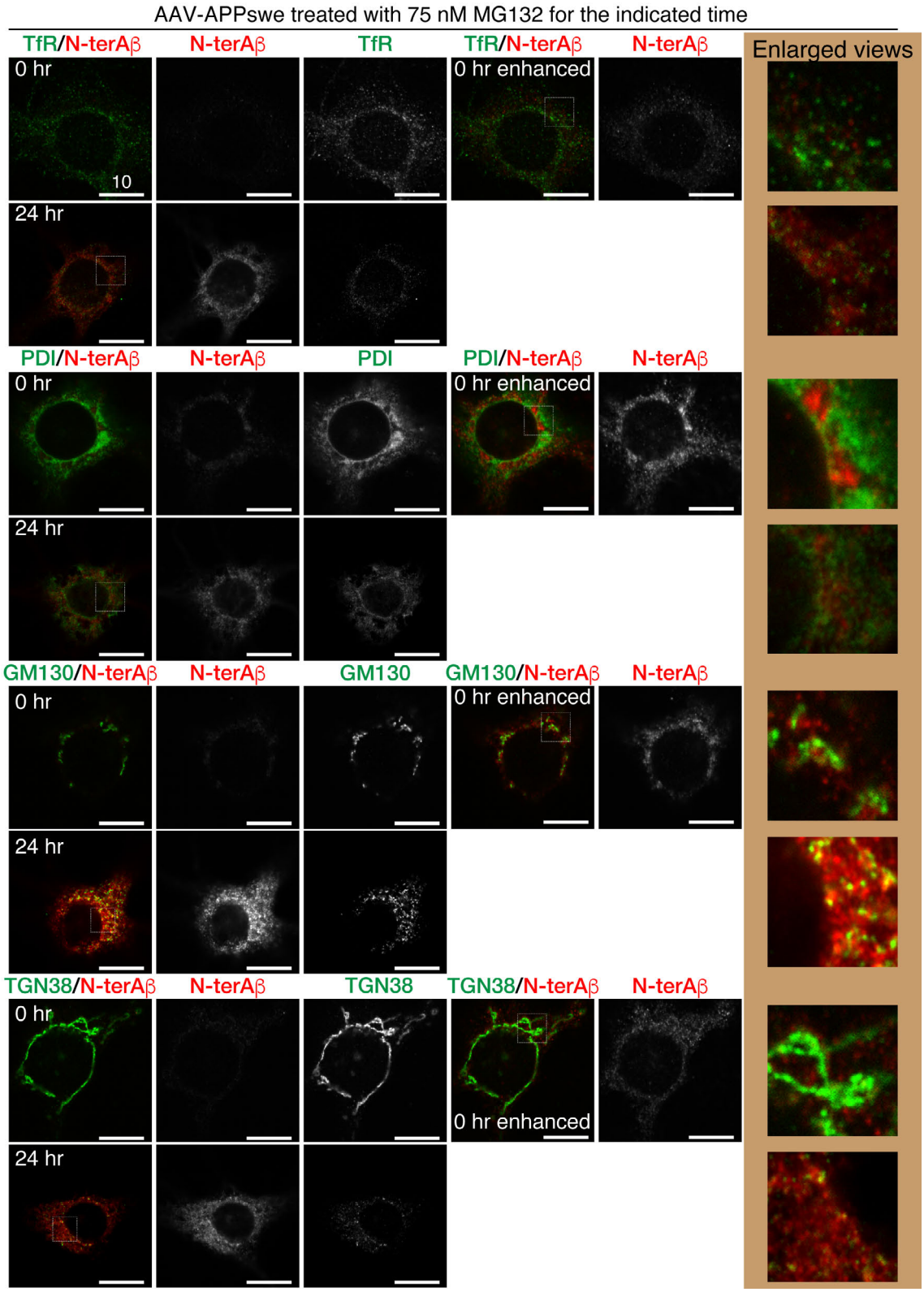
AAV-APPswe treated with 75 nM MG132 for the indicated time
TfR/N-terAβ
N-terAβ
TfR
TfR/N-terAβ
N-terAβ
Enlarged views
0 hr
10
0 hr enhanced
24 hr
PDI/N-terAβ
N-terAβ
PDI
PDI/N-terAβ
N-terAβ
0 hr
0 hr enhanced
24 hr
GM130/N-terAβ
N-terAβ
GM130
GM130/N-terAβ
N-terAβ
0 hr
0 hr enhanced
24 hr
TGN38/N-terAβ
N-terAβ
TGN38
TGN38/N-terAβ
N-terAβ
0 hr
0 hr enhanced
24 hr

Figure S10 Steady-State Distribution of N-terAβ, with or without Proteasome Inhibition, in APPswe-Transduced Mature Neurons, related to Figure 10

APPswe-transduced primary rat hippocampal neuronal cultures were treated with 75 nM MG132 for the indicated time. The cultures were double-stained with anti-ASPD rpASD1 antibody and antibody against organelle marker protein (see Transparent Methods). Representative double-stained images obtained with a highly sensitive, direct photon-counting system with a 100x oil objective lens are shown, along with the corresponding single red or green images. Scale bar = 10 μm. Without proteasome inhibition, the N-terAβ signal is weak. As a reference, red enhanced images are also shown. An enlarged view of the field enclosed by a hatched line is shown on the right. From the red enhanced images, the weak N-terAβ signal appeared to be present together with the ER or the cis-Golgi, but not with the TGN or the RE.

Figure S11

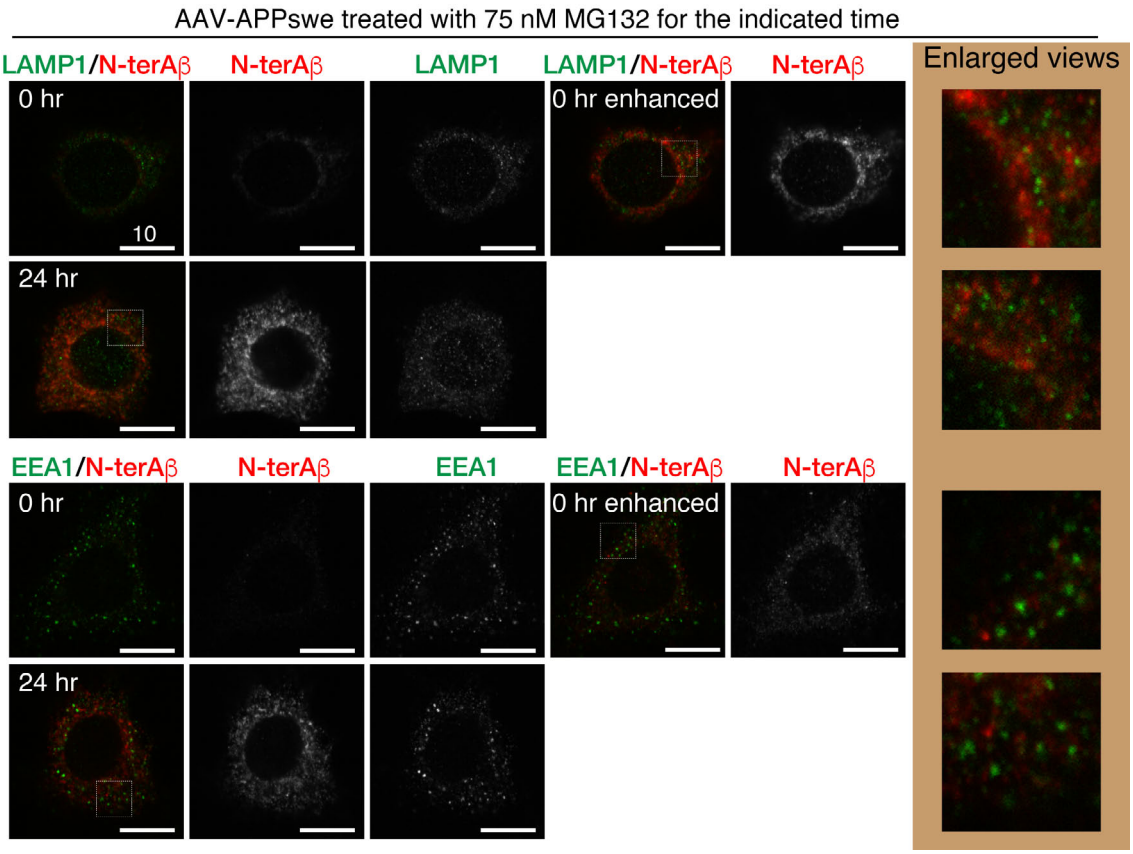

Figure S11 Steady-State Distribution of N-terAβ, with or without Proteasome Inhibition, in APPswe-Transduced Mature Neurons, related to Figure 10

APPswe-transduced primary rat hippocampal neuronal cultures were treated with 75 nM MG132 for the indicated time. The cultures were double-stained with anti-ASPD rpASD1 antibody and antibody against organelle marker protein (see Transparent Methods). Representative double-stained images obtained with a highly sensitive, direct photon-counting system with a 100x oil objective lens are shown, along with the corresponding single red or green images. Scale bar = 10 μm. Without proteasome inhibition, the N-terAβ signal is weak. As a reference, red enhanced images are also shown. An enlarged view of the field enclosed by a hatched line is shown on the right. From the red enhanced images, the weak N-terAβ signal didn't appear to be present together with the EE or the Lys.

Figure S12

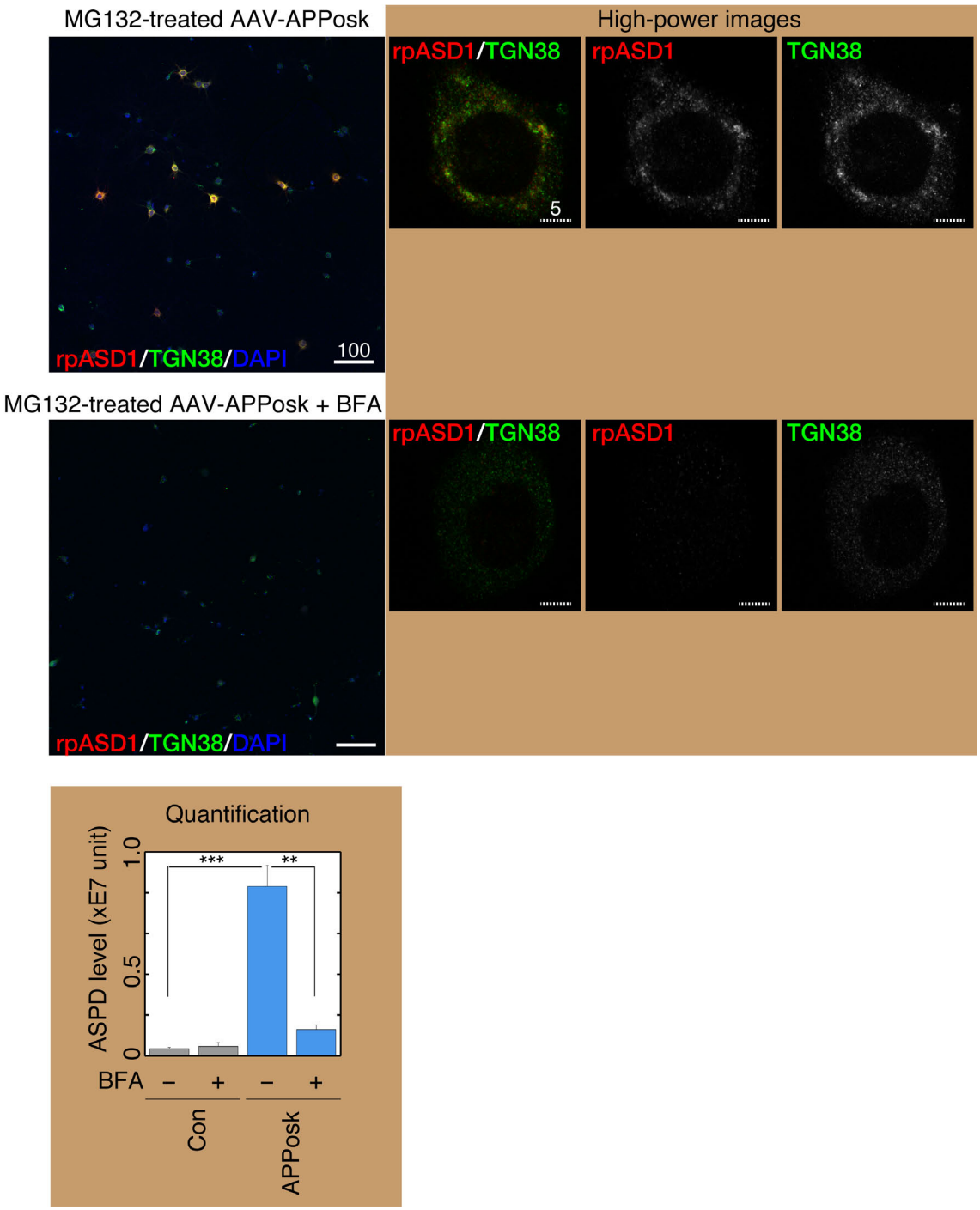

Figure S12 BFA Effects on the TGN in APPosk-Transduced Neurons, related to Figure 11

Primary rat hippocampal neuronal cultures with AAV-APPosk transduction were treated with 75 nM MG132 for 24 hr in the absence or the presence of 0.6 μg/ml BFA,

as in Figure 9. The cultures were triple-stained with rpASD1 antibody, anti-TGN38 (TGN marker) antibody, and DAPI. Representative images are shown with scale bars in μm. The ASPD-staining of each culture was quantified using the In Cell Analyzer (*GE Healthcare Lifesciences*) as in Figure 9 (mean ± SD, n = 3; Scheffé *post hoc* test, ***, $p < 0.0001$; **, $p = 0.0004$). High-power images obtained with a highly sensitive, direct photon-counting system with a 100x oil objective lens are shown on the right. Single red or green images are also shown.

Figure S13

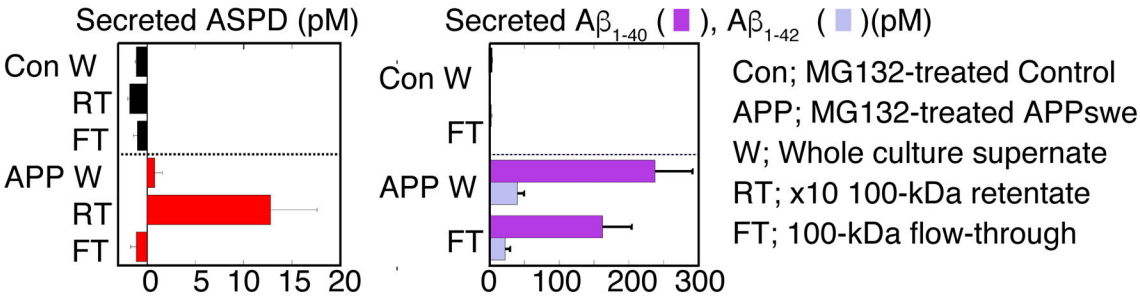

Figure S13 Intra-neuronal ASPD were Secreted and Showed Toxicity, related to Figure 12

The culture supernates were obtained from primary rat hippocampal neuronal cultures, with or without AAV-APPswe transduction, which were treated with 75 nM MG132 for 24 hr as in Figure 12B. $A\beta_{1\text{-}40}$ and $A\beta_{1\text{-}42}$ were quantified by using a WAKO ELISA system (details in Transparent Methods). Mean ± SD, n = 3.

Figure S14

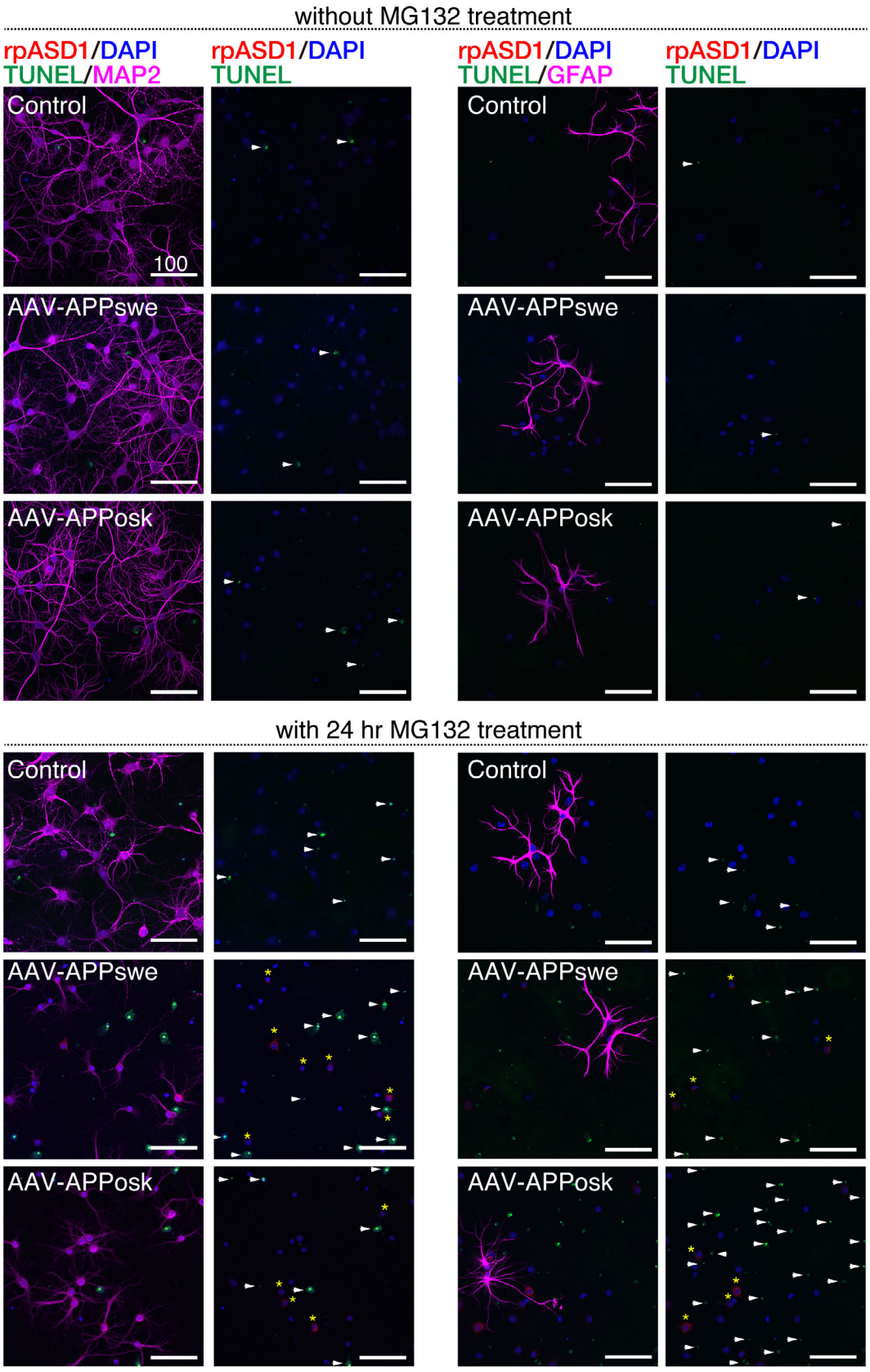
without MG132 treatment
rpASD1/DAPI
TUNEL/MAP2
rpASD1/DAPI
TUNEL
rpASD1/DAPI
TUNEL/GFAP
rpASD1/DAPI
TUNEL
Control
100
AAV-APPswe
AAV-APPosk
with 24 hr MG132 treatment
Control
AAV-APPswe
AAV-APPosk

Figure S14 Secreted ASPD Induced Apoptotic Degeneration of Surrounding Neurons, related to Figure 13

APP-transduced or untransduced control cultures were treated with or without 75 nM MG132 for 24 hr and quadruple-stained with rpASD1, DAPI, TUNEL, and MAP2/GFAP. Representative quadruple-stained images are shown, along with the corresponding triple staining of rpASD1(*), DAPI, and TUNEL (arrowheads) on the right, with 100 μm scale bars.

Figure S15

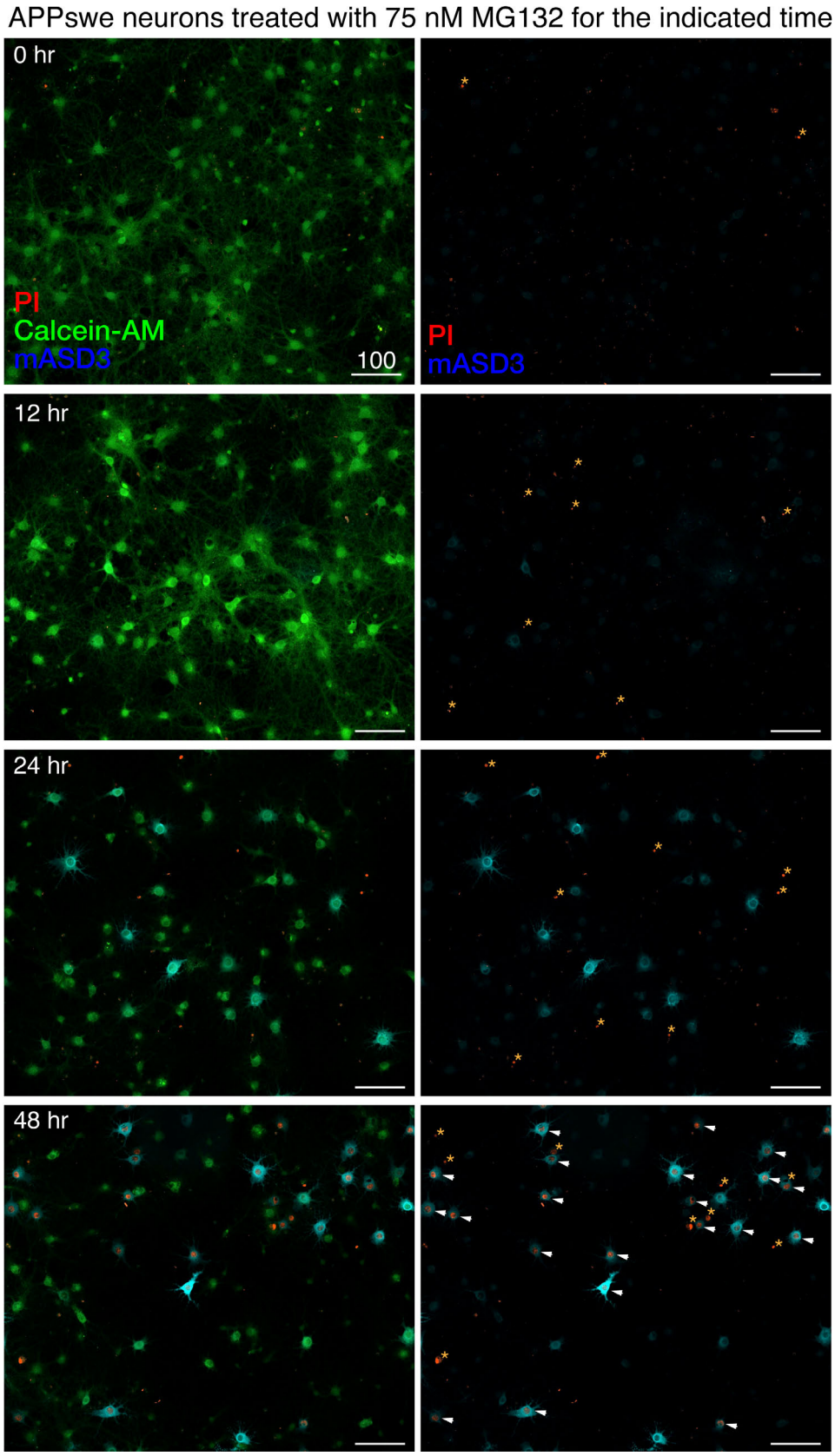
APPswe neurons treated with 75 nM MG132 for the indicated time
0 hr
PI
Calcein-AM
mASD3
100
PI
mASD3
12 hr
24 hr
48 hr

Figure S15 PI-Detectable, Non-Apoptotic Death Occurred in ASPD-Producing Neurons at 48 hr of MG132 Treatment, related to Figure 13

APPswe-transduced primary rat hippocampal neuronal cultures were treated with 75 nM MG132 for the indicated time, triple-stained with propidium iodide (PI), calcein-AM, and anti-ASPD mASD3 antibody (see Transparent Methods), and photographed. Left columns show triple staining and right columns show the corresponding PI/mASD3-staining. Representative images are shown with 100 μm scale bars. Asterisks show apoptotic nuclei detected by PI. Arrowheads show PI-detectable non-apoptotic death in ASPD-producing neurons.

Figure S16

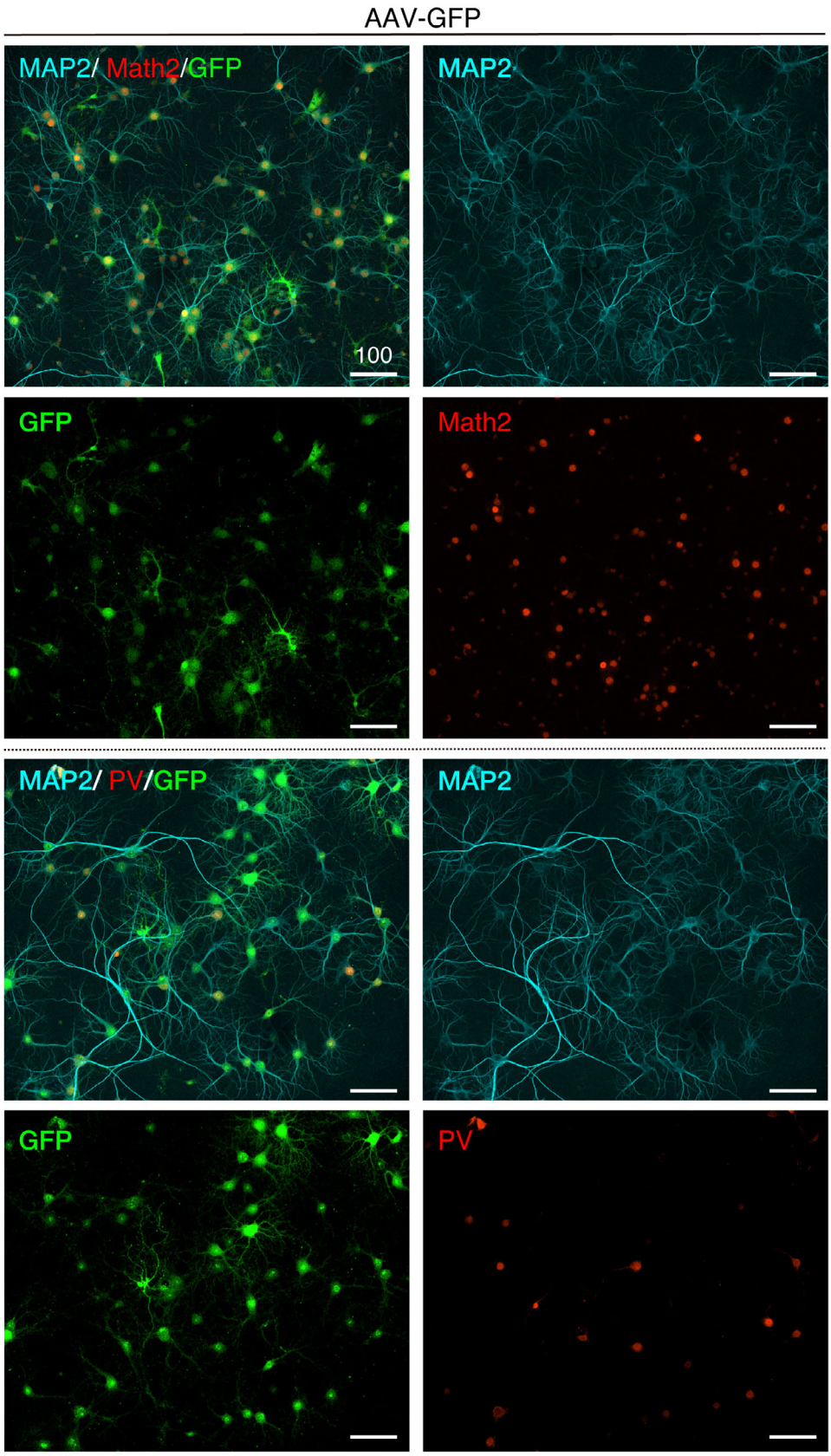
AAV-GFP
MAP2/ Math2/GFP
100
MAP2
GFP
Math2
MAP2/ PV/GFP
MAP2
GFP
PV

Figure S16 GFP was Transduced Both in Excitatory and Inhibitory Neurons with the Same Efficiency, related to Figures 14, S17, and S18

GFP-transduced neuronal cultures without MG132 treatment were triple-stained with MAP2, GFP, and Math2 or PV. Representative images are shown with 100 μm scale bars. Please note that GFP was transduced to almost all neurons, irrespective of Math2-positive excitatory neurons (Schwab et al., 2000) (99.1 ± 1.4 %, n = 30) or parvalbumin (PV)-positive GABAergic interneurons (97.0 ± 3.7 %, n = 30). The ratio of the GFP-containing neurons among either MAP2/Math2- or MAP2/PV-double-positive neurons was quantified using a Yokogawa CQ1 (see Transparent Methods; Inset, mean ± SD).

Figure S17

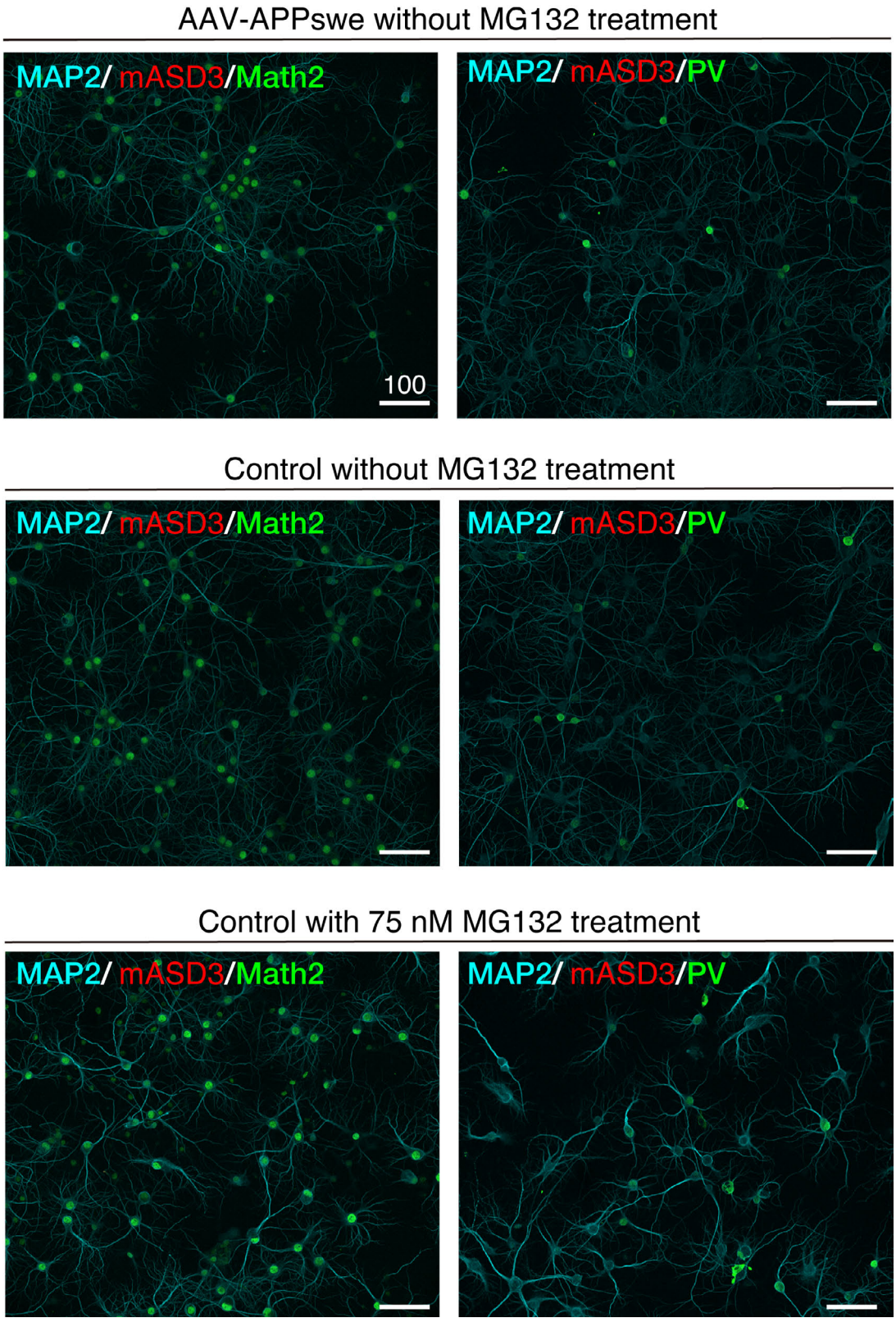
AAV-APPswe without MG132 treatment
MAP2/ mASD3/Math2
MAP2/ mASD3/PV
100
Control without MG132 treatment
MAP2/ mASD3/Math2
MAP2/ mASD3/PV
Control with 75 nM MG132 treatment
MAP2/ mASD3/Math2
MAP2/ mASD3/PV

Figure S17 ASPD Accumulate Only in Excitatory Neurons, related to Figures 14 and S18

APPswe-transduced or untransduced control neuronal cultures were treated with or without MG132 treatment for 24 hr and then triple-stained with MAP2, mASD3, and Math2 or PV. Representative images are shown with 100 μm scale bars.

Figure S18

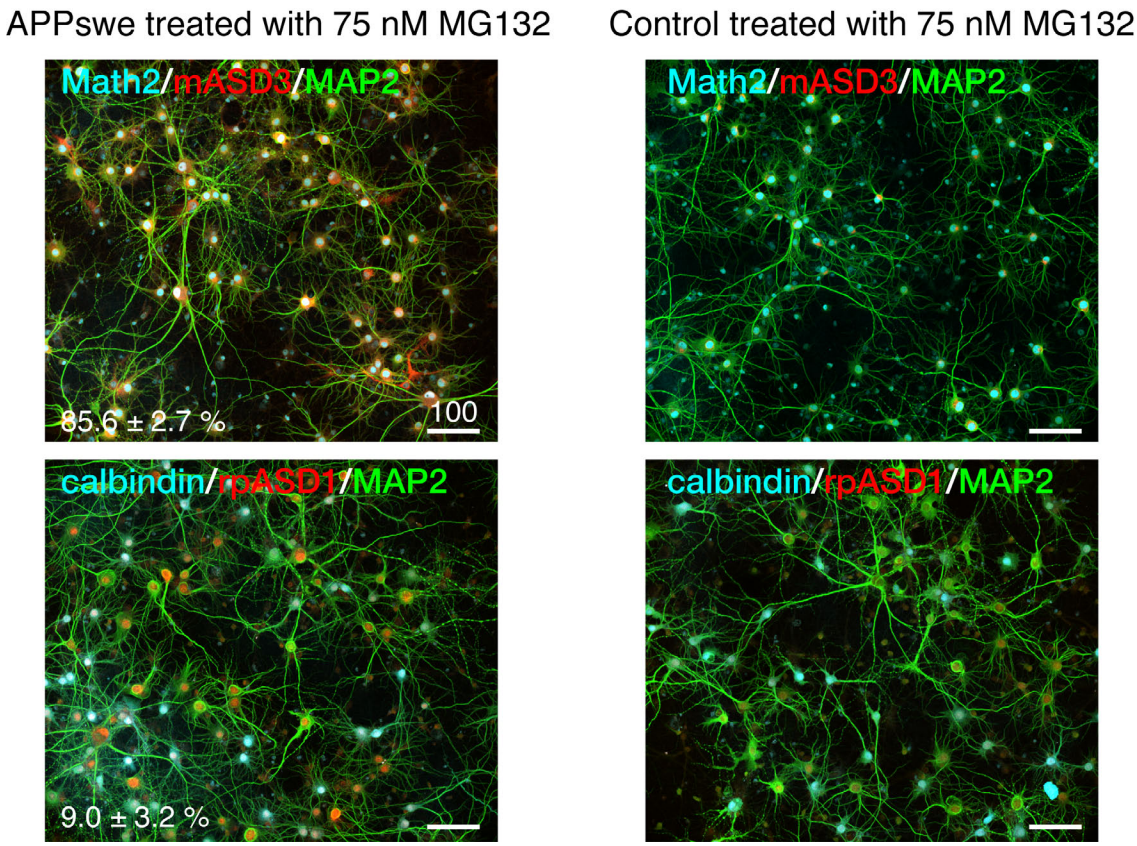

Figure S18 ASPD Accumulate Only in Excitatory Neurons, related to Figure 14

APPswe-transduced or untransduced control neuronal cultures with 24 hr MG132 treatment were triple-stained with MAP2, mASD3, and Math2 or with MAP2, rpASD1, and calbindin. The ratio of the ASPD-containing neurons among either MAP2/calbindin or MAP2/Math2-double-positive neurons was quantified using a Yokogawa CQ1 (see Transparent Methods; Inset, mean ± SD, n = 5). ASPD were detected by anti-ASPD rpASD1 or mASD3 antibody.

Figure S19

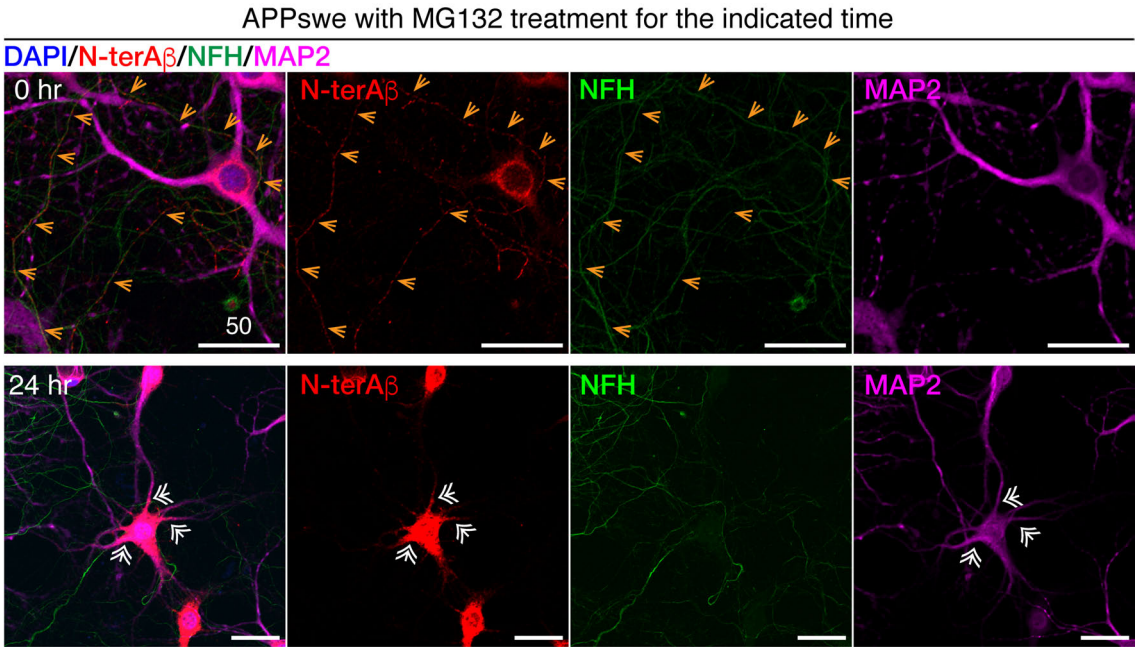

Figure S19 Aβ Distribution in MG132-treated APPswe-transduced Neurons, related to Figure 5

Primary rat hippocampal neuronal cultures with AAV-APPswe transduction were treated with 75 nM MG132 for 24 hr, and quadruple-stained at 22 DIV with the anti-ASPD rpASD1 antibody, anti-NFH antibody, anti-MAP2 antibody, and DAPI (see Transparent Methods). A representative image, along with the corresponding single red, green, or magenta image, is shown with 50 μm scale bars. Orange arrows mark axons, while white double-lined arrows mark dendrites. ASPD were co-localized with NFH (orange arrows) in the upper panels, but co-localized with MAP2 (white double-lined arrows) in the lower panels.

Transparent Methods

Ethics

The Animal Care and Experimentation Committees of MITILS, Kyoto University, FBRI, and TAO approved animal experiments.

Introduction of human APP770 genes bearing early-onset mutations into mature primary neuronal cultures by using an AAV vector

APP exists in several alternatively spliced isoforms, including APP695, APP751, and APP770. APP751 and APP770 contain a Kunitz-type protease inhibitor (KPI) domain (Nalivaeva and Turner, 2013). KPI domain-containing APP770 was used to establish a mature neuron-based system, because reports show that the protein and mRNA levels of KPI domain-containing APP isoforms (in particular APP770) are elevated in AD brains and are associated with increased Aβ deposition (Menendez-Gonzalez et al., 2005; Tanaka et al., 1988). It was also reported that prolonged activation of extrasynaptic NMDA receptor in neurons could shift APP expression from APP695 to KPI domain-containing APP isoforms, accompanied with increased production of Aβ (Bordji et al., 2010). Therefore, an adeno-associated virus 1-derived (AAV) vector expressing human APP770 gene with a familial AD mutation was produced as described previously (Li et al., 2006). The expression cassette contains a cytomegalovirus (CMV) immediate-early promoter, cDNA of human mutant APP, and simian virus 40 polyadenylation signal sequence between the inverted terminal repeats of the AAV2 genome. HEK293 cells were transduced with the vector plasmid, the AAV2 *rep* and AAV1 *vp* expression plasmids, and the adenoviral helper plasmid pHelper (Invitrogen). The recombinant viruses were purified by isolation from two sequential continuous CsCl gradients. Viral titers were determined by measuring the vector genome with quantitative PCR (Li et al., 2006). Primary rat hippocampal cultures were prepared from embryonic day 17 pups and plated at 4.1×10^4 cells/cm^2 (48-well plates), 2.7×10^4 cells/cm^2 (24-well plates), or 3.4×10^4 cells/cm^2 (cover glasses) in Neurobasal media containing B27 supplement and 2.5 μM L-glutamine (termed LC)(Ohnishi et al., 2015). At 10 DIV, the cultures were infected with the above AAV vectors, which were removed at 14 DIV. At 21 DIV, the medium was replaced with fresh LC, with or without MG132 (3175-v), lactacystin (4368-v), or epoxomicin (4381-v) as a proteasome inhibitor (Peptide Institute Inc.), dissolved in sterile

Hybri-Max^{TM} dimethyl sulfoxide (Sigma-Aldrich). Brefeldin A (BFA)(Sigma-Aldrich B5936) was dissolved in LC containing 10% (v/v) ACM.

Evaluation of secreted ASPD toxicity

Two different lines of experiments were performed.

First, to examine whether ASPD secreted from neurons indeed exerted neurotoxicity against neighbouring neurons, AAV-APPswe transduced neurons (see above "Primary neuronal cultures") were pretreated for 2 hr with ASPD-specific mouse monoclonal mASD3 antibody (1 ng/ml), which we have established and shown to specifically block the neurotoxicity of patient-derived ASPD against mature neurons (Noguchi et al., 2009). Then, these neurons were further treated with 75 nM MG132 for 24 hr. As a control, untransduced neurons were treated in the same way.

Second, culture media were collected from untransduced or AAV-APPswe transduced neurons after 24 hr MG132 treatment. The ASPD-specific mASD3 antibody or normal mouse IgG (12 μg each) was covalently conjugated to 60 μl of *N*-hydroxysuccinimide (NHS)-activated magnetic beads (Thermo Scientific) according to the manufacturer's instruction. The collected culture media (1.2 ml) were incubated with the resulting mASD3-conjugated or normal mouse IgG-conjugated magnetic beads by slowly rotating the sample for 1 hr at room temperature (r.t.). Another primary rat hippocampal culture at 22 DIV without AAV transduction was treated with the immunodepleted medium for 24 hr.

In both experiments, the neurons were fixed and immunostained with appropriate antibodies, and quantification of NAKα3-expressing neurons was performed as described below: "Immunocytochemistry."

Immunocytochemistry and quantification

ASPD were detected by immunohistochemical staining with ASPD-specific rpASD1 antibody or mASD3 antibody (Noguchi et al., 2009), which has been used to detect ASPD in immunopathological studies of human brains (Noguchi et al., 2009; Ohnishi et al., 2015). Primary neuronal cultures were fixed with 4% (w/v) paraformaldehyde (PFA) for 15 min at 37 °C and rinsed three times with Dulbecco's phosphate-buffered saline without calcium and magnesium (PBS). The fixed cells were treated with 1 mg/ml $NaBH_4$ for 20 min at r.t., rinsed three times with PBS, permeabilized with 0.2%

(v/v) Triton X-100 for 5 min at r.t., and rinsed three times with PBS. The cells were pretreated with PBS containing 3% (w/v) BSA (Sigma-Aldrich) and 10% (v/v) normal goat serum (NGS)(IBL Co., Ltd.) for 30 min at r.t., and incubated overnight with primary antibody against APP (1:250, Millipore AB5988P), GFAP (1:400, Sigma-Aldrich G3893), MAP2 (1:5000 or 1000, EnCor Biotechnology Inc. CPCA-MAP2; 2 μg/ml, Sigma-Aldrich M4403), Neurofilament heavy polypeptide (NFH) (1:1000, abcam ab7795), ASPD (4.3 μg/ml rabbit polyclonal rpASD1; 1.3 μg/ml mouse monoclonal mASD3), Aβ N-terminal end (1:200, rabbit monoclonal D54D2, Cell Signaling Technology 8243), PDI (1:2000, Affinity BioReagents MA3-019), GM130 (1:100, BD Biosciences 610822), TGN38 (1:100, BD Biosciences 610898), EEA1 (1:300, BD Biosciences 610457), LAMP1 (1:100, Enzo Life Sciences ADI-VAM-EN001-D), TfR (1:1000, monoclonal H68.4, Invitrogen 13-6800), NAKα3 (0.4 μg/ml, Santa Cruz sc-16051-R), parvalbumin (1:250, Novus NB120-11427), calbindin (CB-955)(1:1000, abcam ab82812), Math2 (1:200, abcam ab85824), or Bassoon (1:500, Enzo Life Sciences ADI-VAM-PS003) at 4 °C. After three washes with PBS, the cells were incubated with a highly cross-adsorbed secondary antibody in PBS containing 3% (w/v) BSA and 10% (v/v) NGS (Alexa Fluor 546 (1:1000), Alexa Fluor 555 (1:1000), or Alexa Fluor 594 (1:1000) as anti-rabbit IgG; Alexa Fluor 488 (1:400), Alexa Fluor 555 (1:1000), or Alexa 647 (1:1000) as anti-mouse IgG; Alexa Fluor 405 (1:1000), Alexa Fluor 488 (1:1000) or Alexa Fluor 647 (1:2000) as anti-chick IgG, Molecular Probes) for 90 min at r.t. In some experiments, cells were counterstained with 4',6-diamidino-2-phenylindole (DAPI)(1:500, Dojindo Molecular Technologies, Inc.) along with the secondary antibodies. The cells were rinsed three times with PBS and mounted with Prolong Gold anti-fade reagent (Invitrogen). TUNEL staining was performed using a DeadEnd^{TM} Fluorometric TUNEL System (Promega) according to the manufacturer's instructions. The TUNEL-stained cells were further immunostained with the anti-ASPD rpASD1 antibody, followed by DAPI counterstaining as described above. Live/dead dual cell staining was performed using PI and calcein-AM(Hoshi et al., 2003). Briefly, live cells were incubated with the solution containing PI (1:100, Dojindo Molecular Technologies, Inc.) and calcein-AM (1:500, Dojindo Molecular Technologies, Inc.) for 30 min at 37 °C, and immediately fixed with 10% (v/v) neutral buffered formalin for 30 min at 4 °C, then immunostaining was performed as described above. Low-magnification fluorescence images were acquired

via x10-x20 objective lenses with a cooled CCD camera using photomultiplier tubes on a Zeiss LSM710 confocal microscope with constant laser intensity and signal detection settings (Ohnishi et al., 2015). High-power views were taken with an x100 oil immersion lens using a direct photon-counting ConfoCor 3 avalanche photodiode detection system on a Zeiss LSM710 confocal microscope with constant laser intensity and signal detection settings (Ohnishi et al., 2015). Neuronal images were taken at 0.4 μm intervals on the z-axis. ASPD formation detected by ASPD-specific rpASD1 antibody was quantitated by using a GE Healthcare Life Sciences "IN Cell Analyzer" system. Approximately 500 cells were randomly selected from seven different fields. The weighted colocalization coefficients were obtained using ZEN2009 software (Zeiss) exactly according to the manufacturer's instructions. The weighted colocalization coefficients consider the intensity value of the summed pixels and calculate values based on the estimated fluorophore population. In calculating the weighted colocalization coefficients, all imaging parameters that influence the intensity of the image remain the same for all data acquisitions, including the objective lens, laser power, filter sets, wavelength collections, acquisition speed, camera, and APD settings. The weighted colocalization coefficients represent the number of red pixels (rpASD1 or N-terminal end specific Aβ) that colocalize with green pixels (organelle markers) divided by the total number of red pixels. To quantify NAKα3-expressing neurons, a confocal quantitative image cytometer, CQ1 (Yokogawa Electric Corporation), was used to acquire 4 to 9 view fields/well. The NAKα3 area was calculated from the sum of areas stained by the anti-NAKα3 antibody. Co-localization of ASPD signals with either anti-parvalbumin/anti-calbindin or anti-Math2 signals was also quantitatively determined by using CQ1 as described above.

Viability

Viability was determined with a Cell Counting Kit-8 (Dojindo Molecular Technologies, Inc.) according to the manufacturer's instructions.

In house-developed ASPD CLEIA

ASPD-specific CLEIA was developed with two ASPD-specific antibodies, rpASD1 as a capture antibody and mASD3 as a detection antibody (Noguchi et al., 2009). rpASD1 antibody (500 ng/well) was applied to 96-well microplates, which were incubated

overnight at 4 ˚C, and blocked with 3% (w/v) BSA in TBS for 30 min at r.t. The sample or the standard was added, and incubation was continued for 1 hr at r.t. The plates were washed, mASD3 antibody (100 ng/well) was added, and incubation was continued for 1 hr at r.t. The plates were rewashed and incubated with horseradish peroxidase-conjugated anti-mouse IgG (4 ng/well, Jackson ImmunoResearch Laboratories, Inc. 715-035-151) for 1 hr at r.t. Immunoreactions were detected by incubating the plates with a chemiluminescent substrate (Thermo Fisher Scientific Inc. QL227687) for 1 min in the dark. Luminescence was detected with a Berthold luminometer. ASPD were determined from a standard curve generated from serial dilutions of synthetic ASPD, the concentration of which was pre-determined by quantitative amino acid analysis (Ohnishi et al., 2015). As a negative control, solutions of $A\beta_{1-42}$ containing monomers and LMW-Aβ (such as dimers) were prepared (Ohnishi et al., 2015; Xiao et al., 2015). Briefly, lyophilized $A\beta_{1-42}$ was dissolved in 10 mM NaOH solution to give a 0.6 mM solution, followed by 10-fold dilution with 10 mM phosphate buffer (pH 7.4). The 50-kDa flow-through fraction (Vivaspin 500, Sartorius) obtained by centrifugation at $4.8 \times 10^3 \times g$ for 3 min contained mostly $A\beta_{1-42}$ monomers without pre-formed high-mass aggregates (Ohnishi et al., 2015; Xiao et al., 2015). Its concentration was also determined by quantitative amino acid analysis (Ohnishi et al., 2015). The ASPD-specific CLEIA system did not respond to this 50-kDa flow-through fraction of $A\beta_{1-42}$.

Quantification of ASPD, $A\beta_{1-40}$, and $A\beta_{1-42}$

The culture supernatant was collected and immediately filtered through a 0.22 μm Millex-GV filter. $A\beta_{1-40}$ and $A\beta_{1-42}$ in the supernatant were quantified using the WAKO sandwich ELISA systems specific to $A\beta_{1-40}$ (292-62301) and $A\beta_{1-42}$ (296-64401), respectively, according to the manufacturer's instructions. The 10-times-concentrated culture supernate was obtained from the above 0.22-μm filtered sample by recovering the 100-kDa retentates (Vivaspin 20, Sartorius). This filtration process eliminated Aβ monomers and LMW-Aβ (such as dimers and dodecamers) from the 100-kDa retentates (Noguchi et al., 2009). ASPD in the supernates was quantified using the in house developed ASPD-specific CLEIA system.

TEM

Samples were negatively stained with 4% (w/v) uranyl acetate solution on high-resolution carbon substrate on STEM 100Cu grids (HRC-C10, Okenshouji Co., Ltd) and analyzed immediately (Ohnishi et al., 2015).

Dot blotting

Dot blotting was performed (Ohnishi et al., 2015) using 40 ng/ml ASPD-specific rpASD1 antibody in 5% skim milk with membrane boiling, and 12.5 ng/ml anti-Aβ N-terminal 82E1 antibody in 10% skim milk without membrane boiling. Immunoreactions were detected with SuperSignal West Femto chemiluminescent substrates and quantified using a LAS-4000 Mini (Ohnishi et al., 2015).

ASPD Preparation

ASPD are neurotoxic, spherical Aβ assemblies of 10-15-nm diameter (measured by TEM) that are recognized by ASPD-specific antibodies (Ohnishi et al., 2015). Synthetic ASPD formed in 50 μM $A\beta_{1-42}$ solution (derived from wild-type $A\beta_{1-42}$ or $A\beta_{1-42}$-osk) using in house prepared highly soluble Aβ peptides (essential for obtaining ASPD; see "Aβ synthesis") in F12 buffer without L-glutamine and phenol red by slowly rotating the solution for ~16 hr at 4 ˚C (Ohnishi et al., 2015). ASPD quality was confirmed by dot blotting, TEM, amino acid analysis, and toxicity assays (Ohnishi et al., 2015).

Aβ synthesis

Highly soluble $A\beta_{1-42}$ and $A\beta_{1-42}$-osk peptides were synthesized in house, purified, finally lyophilized in a solution containing 0.1% (v/v) TFA and 30% (v/v) acetonitrile on ice (~150 μM), and kept at -30 ˚C (Ohnishi et al., 2015). Purity was confirmed by analytical HPLC, quantitative amino acid analysis, and matrix-assisted laser desorption/ionization time of flight/mass spectrometry. The peptides were completely dissolved in 1,1,1,3,3,3 hexafluoro-2-propanol (HFIP for HPLC; Kanto Chemical Co., Inc.) at ~80 μM and lyophilized (~40 nmol/tube)(Ohnishi et al., 2015). This step was repeated three times. The lyophilized peptide was kept at -30 ˚C. We have long used HFIP from Sigma-Aldrich, which we previously found contained ~1.3 mM bis(2-ethylhexyl)phthalate (DEHP)(Ohnishi et al., 2015). This means that solutions of peptide lyophilized in Sigma-Aldrich HFIP usually contained ~0.65 mM DEHP when the peptide concentration was 50 μM. Therefore, when we used HFIP in which DEHP

was undetectable, we added DEHP (0.65 mM final concentration; Tokyo Chemical Industry Co., Ltd.)(Ohnishi et al., 2015) to ensure consistency with our previous conditions (Hoshi et al., 2003; Matsumura et al., 2011; Noguchi et al., 2009).

Western blotting

Whole-cell lysates were prepared by lysing the cells in a lysis buffer (50 mM Tris (pH 7.5), 107 mM NaCl, 5 mM EDTA, 0.1% SDS, 0.5% sodium deoxycholate, 1% NP40, 1 μg/mL pepstatin, and 1x EDTA-free complete protease inhibitor cocktail (Roche)) and collecting the supernatant by centrifugation (Ohnishi et al., 2015). In detecting APP, the supernatant (10 μg/lane) was separated under denaturing conditions on reducing NuPAGE 4-20% Tris-Glycine gels and transferred onto a 0.2-μm nitrocellulose membrane. The membrane was blocked with 5% (w/v) skim milk for 1 hr at r.t., followed by incubation with primary antibody (0.1 μg/ml anti-APP, IBL11090; 0.3 μg/ml anti-actin, Millipore MAB1501R). In detecting Aβ, the supernatant (8 μg/lane) was separated under denaturing conditions on reducing NuPAGE 4-12% Bis-Tris gels (Invitrogen) and transferred onto a 0.2-μm nitrocellulose membrane. The membrane was blocked with 5% (w/v) skim milk for 1 hr at r.t., followed by incubation with primary antibody (0.05 μg/ml anti-Aβ N-terminal end, CST8243; 0.3 μg/ml anti-actin). In both cases, bands were detected with Super Signal West Femto and quantified using a LAS-4000 Mini (Ohnishi et al., 2015).

Statistical Analyses.

Statistical significance was assessed at the 5% significance level using Scheffé *post hoc* tests with StatView®5 software.

Supplemental References

Bordji, K., Becerril-Ortega, J., Nicole, O., and Buisson, A. (2010). Activation of Extrasynaptic, But Not Synaptic, NMDA Receptors Modifies Amyloid Precursor Protein Expression Pattern and Increases Amyloid-β production. J. Neurosci. *30*, 15927-15942.

Hoshi, M., Sato, M., Matsumoto, S., Noguchi, A., Yasutake, K., Yoshida, N., and Sato, K. (2003). Spherical aggregates of β-amyloid (amylospheroid) show high neurotoxicity and activate tau protein kinase I/glycogen synthase kinase-3β. Proc. Natl. Acad. Sci. U. S. A. *100*, 6370-6375.

Li, X.G., Okada, T., Kodera, M., Nara, Y., Takino, N., Muramatsu, C., Ikeguchi, K., Urano, F., Ichinose, H., Metzger, D.*, et al.* (2006). Viral-mediated temporally controlled dopamine production in a rat model of Parkinson disease. Mol. Ther. *13*, 160-166.

Matsumura, S., Shinoda, K., Yamada, M., Yokojima, S., Inoue, M., Ohnishi, T., Shimada, T., Kikuchi, K., Masui, D., Hashimoto, S.*, et al.* (2011). Two distinct amyloid β-protein (Aβ) assembly pathways leading to oligomers and fibrils identified by combined fluorescence correlation spectroscopy, morphology, and toxicity analyses. J. Biol. Chem. *286*, 11555-11562.

Menendez-Gonzalez, M., Perez-Pinera, P., Martinez-Rivera, M., Calatayud, M.T., and Blazquez Menes, B. (2005). APP Processing and the APP-KPI Domain Involvement in the Amyloid Cascade. Neurodegener. Dis. *2*, 277-283.

Nalivaeva, N.N., and Turner, A.J. (2013). The amyloid precursor protein: a biochemical enigma in brain development, function and disease. FEBS Lett. *587*, 2046-2054.

Nebenfuhr, A., Ritzenthaler, C., and Robinson, D.G. (2002). Brefeldin A: Deciphering an Enigmatic Inhibitor of Secretion. Plant Physiol. *130*, 1102-1108.

Noguchi, A., Matsumura, S., Dezawa, M., Tada, M., Yanazawa, M., Ito, A., Akioka, M., Kikuchi, S., Sato, M., Ideno, S.*, et al.* (2009). Isolation and characterization of patient-derived, toxic, high mass amyloid β-protein (Aβ) assembly from Alzheimer disease brains. J. Biol. Chem. *284*, 32895-32905.

Ohnishi, T., Yanazawa, M., Sasahara, T., Kitamura, Y., Hiroaki, H., Fukazawa, Y., Kii, I., Nishiyama, T., Kakita, A., Takeda, H.*, et al.* (2015). Na, K-ATPase α3 is a death target of Alzheimer patient amyloid-beta assembly. Proc. Natl. Acad. Sci. U. S. A. *112*, E4465-4474.

Schwab, M.H., Bartholomae, A., Heimrich, B., Feldmeyer, D., Druffel-Augustin, S., Goebbels, S., Naya, F.J., Zhao, S., Frotscher, M., Tsai, M.J.*, et al.* (2000). Neuronal basic helix-loop-helix proteins (NEX and BETA2/Neuro D) regulate terminal granule cell differentiation in the hippocampus. J. Neurosci. *20*, 3714-3724.

Tanaka, S., Nakamura, S., Ueda, K., Kameyama, M., Shiojiri, S., Takahashi, Y., Kitaguchi, N., and Ito, H. (1988). THREE TYPES OF AMYLOID PROTEIN PRECURSOR mRNA IN HUMAN BRAIN: THEIR DIFFERENTIAL EXPRESSION IN ALZHEIMER'S DISEASE. Biochem. Biophys. Res. Commun. *157*, 472-479.

Xiao, Y., Ma, B., McElheny, D., Parthasarathy, S., Long, F., Hoshi, M., Nussinov, R., and Ishii, Y. (2015). Aβ(1-42) fibril structure illuminates self-recognition and replication of amyloid in Alzheimer's disease. Nat. Struct. Mol. Biol. *22*, 499-505.